ITERATOR: A 3D Gait Identification from IR-UWB Technology

Soumya Prakash Rana, Maitreyee Dey, Mohammad Ghavami, and Sandra Dudley
Center for Biomedical Engineering and Communications (BiMEC), School of Engineering,
London South Bank University, London, United Kingdom
Email: ranas9@lsbu.ac.uk

***Abstract*—A more locally cared for and self-managing aging population along with better attention to health-care issues, has resulted in increasing need for non-intrusive monitoring. Wearable and wireless physiological sensors are consistently employed gaining attention over several years. Wearable devices can pose issues such as user privacy, security and discomfort which may have a negative impact on consumer confidence and uptake. Cameras for example are being used but come with the loss of privacy and resulting high computational complexity. A non-contact, non-intrusive 3D human motion model is proposed for the first time for gait disorder identification from impulse radio ultra-wide band (ITERATOR) with the understanding of spherical trigonometry and vector field. The system is compared using the Kinect Xbox One sensor system. The experiment comprises twenty-four human participants where, twenty people have normal walking pattern and four persons have spasticity. The height of different body sections from the ground have been recorded for each individual. The participants have been asked to walk back and forth in front of the UWB radar and simultaneously fixed Kinect Xbox One sensor. The proposed work has transformed the radars backscattered responses through trigonometry and vector algebra where, only vector algebra has been implemented to transform the skeletal data obtained from Kinect. Angles between two thighs have been determined from the proposed UWB algorithm and validated against angles obtained from the Kinect skeletal data. Root mean square error (RMSE) has been measured between proposed UWB prototype and Kinect sensor results with a results RMSE result of less than 0.5.**

***Index Terms*—Gait analysis, Impulse radio ultra-wide band (IR-UWB), Spherical trigonometry, Kinect sensor .**

I. Introduction

Human gait is a bipedal, biphasic, and forward propulsive locomotion of human body where, different body segments coordinate simultaneously. Gait analysis refers the systematic study of that bipedal locomotion which is worthwhile in the medical issues affect human locomotor system or walk. Over past few years, interest in this area has grown, and the gait analysis research has been employed to improve athlete performance [1], monitor patient healing progress [2], help in cases of Parkinsons disease [3] [4], and recognize individuals through their unique walking pattern [5]. The study poses the subjective evaluation by expert observer and quantitative evaluation by equipment for measuring gait parameters such as, step length, stride length, knee angles, etc. Measurement and analysis of these parameters drive the doctors and clinicians to plan their diagnosis and treatment decisions. The most common methods for analyzing gait use force sensitive resistors (FSR) and wearable sensors (WS) or markers.

FSRs are a type of non-wearable sensor (NWS). FSRs are only useful for acquiring contact timing between lower limbs and ground [6] [7]. Popular WSs are force sensors (FS), accelerometers, gyroscopes, extensometers, goniometers, electromyography, active markers, etc. and they are well known for rendering more gait related information such as, angular velocity of stance and swing leg [8], information about heel-strike and toe-off [9], angles between knees, ankles, hips, and foots [10]. Some research has also experimented human gait using continuous wave (CW) radar for authentication purposes [11]. Although, NWS and WS systems provide accurate results, they are restricted by the cost of experimental set-up and intrusiveness respectively [12]. Thus, the medical field must look towards alternative solutions which, are inexpensive, reliable in users homes and do not hamper participants privacy [13].

Thus, the proposed work focuses on to the design and implementation of a noncontact and non-intrusive wireless gait analysis tool ITERATOR. The IR-UWB radar has been chosen for this study that transmits short pulses that enable the system to be employed in multi-path environments. The study is the first work, which would analyze human gait in 3D space from IR-UWB sensing. The model has transformed the back-scattered pulses by implementing trigonometric approach to measure the range, height, and deviation of moving object from the antenna north beam. Subsequently, the height of different body sections have been measured before UWB gait data collection for each individuals which, have been later used to differentiate the lower limbs from upper limbs. Then, vector algebra has been employed to determine the angles between alternative thighs, which is a significant parameter to characterize human gait. Simultaneously, Kinect Xbox One sensor has been used for the validation of the proposed method. Kinect system is a well-known, camera based, and popular sensor for body posture measurement and have been employed for gait analysis by several researchers [14]. However, Kinect is limited to intrusiveness for its camera sensor. So, that the proposed work would be powerful alternative for gait analysis. RMSE has been determined between the results measured from proposed prototype against

Kinect to check the efficiency of the work.

The remaining sections of the article are organised as follows; the laboratory set-up, UWB data acquisition, and the proposed methodology with related radar principles has been detailed in Section II. The description about the Kinect sensor and data interpretation procedure has been provided in Section III. Section IV includes the illustration on RMSE calculation process, experimental results have been demonstrated in Section V. Section VI concludes the paper and provides future research directions for this innovative work.

II. Methods

A graphic representation of the proposed work is shown in Figure 1. Here, only anechoic chamber environment has been considered for the experiment at the current stage. Initially, the radar has been configured and the raw radar scan data have been acquired through the radar application program interface (RAPI). Module service is also configured to retrieve detection information from the environment. The data then have been processed through radar rang principle and proposed elevation and azimuth angle. Finally, the thigh angle has been determined by implementing vector algebra with the help of range, elevation angle, and azimuth angle. Each theoretical backgrounds have been detailed in the following sections.

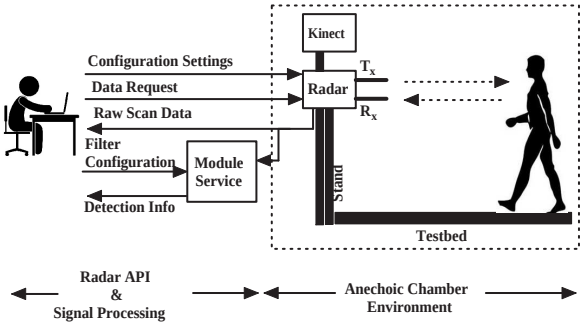

Fig. 1: Schematic diagram of the proposed system.

A. Laboratory Set-up

A Time Domain PulsON 410 ranging and communications module (P410 RCM) and P410 monostatic radar module (P410 MRM) has been utilized for this and previous work by the team [15]–[17], are shown in Figure 2a. The device is a UWB monostatic pulsed Doppler radio transceiver with one transmitter and one receiver antenna. The architecture utilizes two-way time-of-flight (TW-TOF) range measurement techniques and is used here as hybrid ranging radio and a radar sensor device for studying the human gait. The P410 MRM uses monostatic radar module with omni-directional antennas. The device has been configured before data collection in anechoic chamber environment (shown in Figure 2b). It transmits RF from lower limit of frequency 3.1 GHz to upper limit of frequency 5.3 GHz, with the centre frequency at 4.3 GHz by following the Federal Communications Commission (FCC) restrictions [18] for power. Transmission power to the antenna port is specified as -12.64 dBm for safe RF transmission, which abides with FCC regulations [18]. The scan time window for this experiment is 27.57 nanoseconds (ns) long, but the first 5 ns of the waveform contains noise because of the direct path interference between transmitter and receiver antenna, hence the waveform during the first 5 ns is filtered out. The scan interval is set to 25000 μs. The received reflected waveforms are sampled in steps of 61 picoseconds, which results the sampling frequency $f_s = 16.39\ GHz$, with a Pulse Repetition Interval (PRI) of approximately 100 ns.

B. Experimental Data Acquisition

Data have been collected in anechoic chamber which is a non-reflective, non-echoing or echo-free room. The length of the test bed is 3 meters. Twenty four human participants (twenty people having normal walking pattern and four people having spasticity) were involved in this data collection process. Full ethical approval (Reference Number: Eng 01Dec2017) was gained from London South Bank University, where the research code of practice and ethical guidelines are governed by the university ethics panel (UEP). All procedures performed in this study were in accordance with the ethical standards of the institutional and/or national research committee and with the 1964 Helsinki declaration and it's later amendments or comparable ethical standards. Initially, gender and anatomical information (height, length of the limbs) have been recorded for each individual.

(a) P410Device.

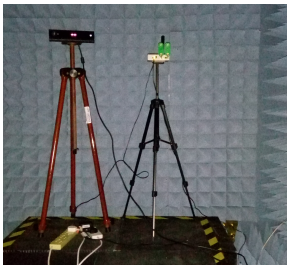

(b) Simultaneous use of P410 UWB radar and Kinect Xbox One sensor for the experiment.

Fig. 2: Devices and anechoic chamber environment.

C. Range and Velocity

The target range R is determined by the TW-TOF of the received pulses. Thus, the range of any physiological movement has been determined by $R = \frac{c\triangle T}{2}$ where, $c = 3 \times 10^8$ meter/seconds is the speed of light, and $\triangle T$ is the propagation delay(s) of the received pulse. The range R decreases when the person comes closer to the radar and and vice versa. The range R has been determined at different time t_1, t_2 and transformed using trigonometry in the following section.

D. Azimuth and Elevation Angles

To differentiate the lower limb, upper limb, and body sections, height has been calculated and used here. Azimuth and elevation angles are significant to define 3D space and calculate the height, range, and arc from radar beam angle. Thus, a 3D scenario has been considered in Figure 3 to obtain elevation and azimuth angle at different time and all the ranges have been denoted here by vector notation as they have a particular direction at a time. Here, O is considered as the radar receiver fixed at a point of height $\overrightarrow{OP}$ from the ground. Triangles ΔOAB, $\Delta OAB'$, ΔOCB, and $\Delta OCB'$ have been drawn from the received radar pulses. Therefore, $\overrightarrow{BC}$ and $\overrightarrow{CB'}$ represent the height of a moving object from the radar line of sight (LOS) $\overrightarrow{OA}$. The moving body section is elevated from the radar LOS at an angle θ and below the LOS at an angle θ'. Here, $\Delta OAB \cong \Delta OAB'$ and $\Delta OCB \cong \Delta OCB'$, therefore the height $\overrightarrow{BC}$ and $\overrightarrow{CB'}$ can be determined from the trigonometric understanding. Let, the angle between $\overrightarrow{BC}$ and $\overrightarrow{OB}$ be α from ΔOAB. The ranges are $\overrightarrow{OA}$, $\overrightarrow{OB}$, and $\overrightarrow{OB'}$ for the propagation delays of t_1, t_2 and t_2' by the pulses, where $t_1 > t_2$, $t_1 > t_2'$ and $\overrightarrow{OA} > \overrightarrow{OB}$, $\overrightarrow{OA} > \overrightarrow{OB'}$. Therefore, the change in range is $(\overrightarrow{OA} - \overrightarrow{OB}) = \Delta d$, the change in propagation delay is $(t_1 - t_2) = \Delta t$, and speed of light or pulse is c. Therefore, pulse can travel the distance in Δt is $\overrightarrow{BC} = \Delta t \times c$. From the right triangle ΔOCB, $\overrightarrow{BC} = \overrightarrow{OB} \times \cos\alpha$. Thus, the height of the moving body section from the radar receiver is $\overrightarrow{OB} \times \cos\alpha$. The UWB radar has been fixed to a certain height of $\overrightarrow{OP'}$, thus the actual height of that moving object from the ground h would be defined by,

$$h = |\overrightarrow{OB} \times \cos\alpha - \overrightarrow{OP'}| \tag{1}$$

Now, the azimuth angle has been determined for measuring orientation of moving body section from radar beam angle (shown in Figure 3). The spherical system measures azimuth angle in a counter clockwise direction from the north beam angle of the radar receiver. Let, the moving limb is deviated at an angle ϕ, where the ranges are $\overrightarrow{OA}$ and $\overrightarrow{OC}$ in propagation delay t_1, t_2. So, the change in range is $(\overrightarrow{OA} - \overrightarrow{OC}) = \overrightarrow{DA}$ at the time interval $(t_1 - t_2) = \Delta t$. The object is deviated from the exact north of the receiver. Now, $\overrightarrow{DA}$ is approximately equivalent to the arc AC created by the object at angle ϕ. Therefore, ϕ is calculated from the radian measure, and equivalent degree conversion is,

$$\phi = \frac{\overrightarrow{DA} \times 360^\circ}{\overrightarrow{OA} \times 2 \times \pi} \tag{2}$$

Therefore, the coordinate of a pulse reflecting from a human body has been found with the help of range, elevation, and azimuth calculation. Let, a pulse has back-scattered from human body when it's arc, range, height are a, r, h respectively. Thus, each pulse has it's coordinate and direction when back-scatters from any physiological movement which allow the points to be considered as vector such as, $a\hat{i} + r\hat{j} + h\hat{k}$ where, $\hat{i}$, $\hat{j}$, and $\hat{k}$ are unit vectors of three planes in a 3D space. The subscripts of a, r, and h have been used through out the paper to denote arc, range, and height of a back-scattered pulse. The height of a back-scattered pulse has been considered here with the a priori knowledge of body sections to differentiate the lower limb from upper limb. The back-scattered pulses within the height of lower limb has been considered here to determine angles between alternative thighs and detailed in the following sections.

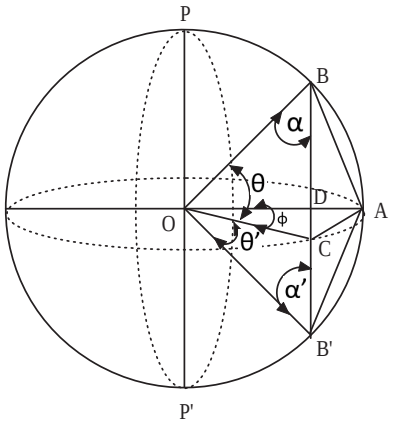

Fig. 3: Elevation and azimuth angle during the gait.

E. Angle between thighs

The angles between two alternative thighs are pivotal parameters for characterization of gait [19]. Thighs are connected through pelvis via the ball-socket and femoral head bearing human body weight and the force of the strong muscles of the hip and leg. Therefore, the angle between thighs changes during the extension and flexion movements. Here, two random points $\overrightarrow{L_T} = a_1\hat{i} + r_1\hat{j} + h_1\hat{k}$, $\overrightarrow{R_T} = a_2\hat{i} + r_2\hat{j} + h_2\hat{k} \in \mathbb{R}^3$ Euclidean space at time t have been assumed on the left and right thighs respectively (shown in Figure 4) where, the extension of these two vectors towards infinity intersect at human pelvis joint. Thus, the acute angle between these vectors has been identified by employing vector dot product and denoted by δ. The derivation of δ has been demonstrated in Eq. 3.

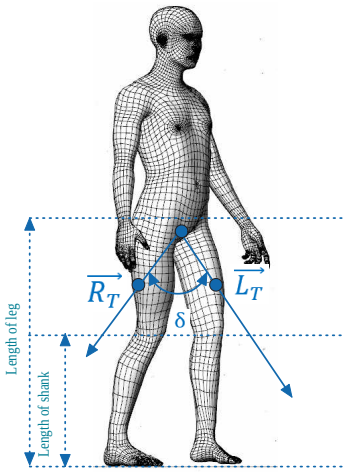

Fig. 4: Consideration of vector while a person is walking.

$$
\begin{aligned}
\overrightarrow{L_T}.\overrightarrow{R_T} &= |\overrightarrow{L_T}||\overrightarrow{R_T}|\cos\delta \\
\Rightarrow \cos\delta &= \frac{\overrightarrow{L_T}.\overrightarrow{R_T}}{|\overrightarrow{L_T}||\overrightarrow{R_T}|} \\
\Rightarrow \cos\delta &= \frac{(a_1\hat{i}+r_1\hat{j}+h_1\hat{k}).(a_2\hat{i}+r_2\hat{j}+h_2\hat{k})}{|a_1\hat{i}+r_1\hat{j}+h_1\hat{k}||a_2\hat{i}+r_2\hat{j}+h_2\hat{k}|} \\
\Rightarrow \cos\delta &= \frac{(a_1a_2+r_1r_2+h_1h_2)}{\sqrt{a_1^2+r_1^2+h_1^2}\sqrt{a_2^2+r_2^2+h_2^2}} \\
\Rightarrow \quad \delta &= \cos^{-1}\left(\frac{(a_1a_2+r_1r_2+h_1h_2)}{\sqrt{a_1^2+r_1^2+h_1^2}\sqrt{a_2^2+r_2^2+h_2^2}}\right)
\end{aligned} \tag{3}
$$

III. Validation via Kinect Xbox One

The outcomes of the proposed work have been validated through the Microsoft Kinect Xbox One. It includes 3D imaging and employs time-of-flight (TOF) technology to deliver high resolution, low latency, light independent 3D image sensing [20]. Kinect captures 3D human motion and track skeleton of human body using color and depth sensor. The proposed work aims to characterize human gait in a non-intrusive manner so, the device has been calibrated to obtain color and skeleton only from the video. Frames per second (FPS) has been fixed at 30 for color and depth sensor for video acquisition. The camera has the field view of 70° horizontal and 60° vertical operates at range from 0.8 to 4.2 meters from the device. It tracks skeleton from moving body posture (as shown in Figure 5) and provides 3D joint coordinates. The Kinect sensor delivers 20 skeletal data (3D joint coordinates) at standing and 10 skeletal data at sitting condition from body posture. This skeletonization process is pretty much similar to the proposed prototype which allows to validate the work through Kinect sensor. Figure 5b shows the 20 joints (white markers) from a human body where, the validation process has used only four joints from lower limb of a human body such as, hip left ($\overrightarrow{HL}$), knee left ($\overrightarrow{KL}$), hip right ($\overrightarrow{HR}$), knee right ($\overrightarrow{KR}$). Then the vector algebra has been employed on these joints to determine angles between thighs and validate the proposed outcomes.

Let, the vectors $\overrightarrow{HL}$, $\overrightarrow{KL}$, $\overrightarrow{HR}$, $\overrightarrow{KR} \in \mathbb{R}^3$. The component form of these vectors have been denoted as, $\overrightarrow{HL} = a_3\hat{i} + r_3\hat{j} + h_3\hat{k}$, $\overrightarrow{KL} = a_4\hat{i} + r_4\hat{j} + h_4\hat{k}$, $\overrightarrow{HR} = a_5\hat{i} + r_5\hat{j} + h_5\hat{k}$, $\overrightarrow{KR} = a_6\hat{i} + r_6\hat{j} + h_6\hat{k}$ where, subscripts with a, r, h represents the distance from $\hat{i}$, $\hat{j}$, $\hat{k}$ planes respectively. These vectors have been further used to determine angle between alternative thighs for gait characterization in the following sections.

(a) Video frame from color sensor.

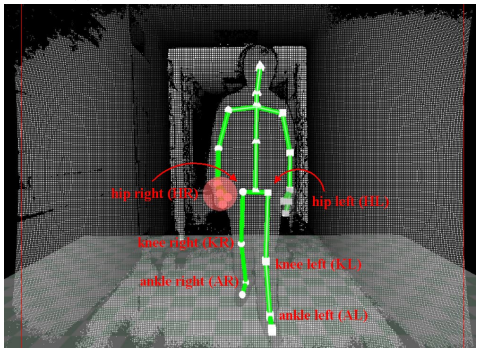

(b) Video frame from depth sensor (i.e., skeleton).

Fig. 5: Sample video frame of human gait tracked through Kinect color and depth sensor.

A. Angle between thighs from Kinect

The angle between thighs has been defined and calculated by the proposed prototype earlier. Now, the angle between thighs has been measured using the hip joints $\overrightarrow{HL}$, $\overrightarrow{HR}$, $\overrightarrow{KL}$, and $\overrightarrow{KR}$ obtained from Kinect skeletal data. Therefore, the two lines are required to calculate the acute angle or the angle of thighs between left and right thigh. Thus, the connecting line between two vectors $\overrightarrow{HL}$ and $\overrightarrow{KL}$ would be spanned by a vector $\overrightarrow{L_{Tk}} = (a_3 - a_4)\hat{i} + (r_3 - r_4)\hat{j} + (h_3 - h_4)\hat{k}$ which represents the space of left thigh. Similarly, the position vector of right thigh $\overrightarrow{R_{Tk}} = (a_5 - a_6)\hat{i} + (r_5 - r_6)\hat{j} + (h_5 - h_6)\hat{k}$. The acute angle between $\overrightarrow{L_{Tk}}$ and $\overrightarrow{R_{Tk}}$ has been determined by their dot product and denoted by $\delta\,'$ (detailed in Eq. 4)

where, $(a_3 - a_4) = a_{34}$, $(r_3 - r_4) = r_{34}$, $(h_3 - h_4) = h_{34}$, $(a_5 - a_6) = a_{56}$, $(r_5 - r_6) = r_{56}$, $(h_5 - h_6) = h_{56}$ have been considered for simplification of the calculations.

$$\begin{aligned}
\overrightarrow{L_{Tk}}.\overrightarrow{R_{Tk}} &= |\overrightarrow{L_{Tk}}||\overrightarrow{R_{Tk}}| \cos\delta\,' \\
\Rightarrow \cos\delta\,' &= \frac{\overrightarrow{L_{Tk}}.\overrightarrow{R_{Tk}}}{|\overrightarrow{L_{Tk}}||\overrightarrow{R_{Tk}}|} \\
\Rightarrow \cos\delta\,' &= \frac{(a_{34}\hat{i} + r_{34}\hat{j} + h_{34}\hat{k}).(a_{56}\hat{i} + r_{56}\hat{j} + h_{56}\hat{k})}{|a_{34}\hat{i} + r_{34}\hat{j} + h_{34}\hat{k}||a_{56}\hat{i} + r_{56}\hat{j} + h_{56}\hat{k}|} \\
\Rightarrow \cos\delta\,' &= \frac{a_{34}a_{56} + r_{34}r_{56} + h_{34}h_{56}}{\sqrt{a_{34}^2 + r_{34}^2 + h_{34}^2}\sqrt{a_{56}^2 + r_{56}^2 + h_{56}^2}}
\end{aligned} \tag{4}$$

IV. Quantitative scoring via RMSE

Root mean squared error (RMSE) is a quadratic measurement between the outcomes which determine the magnitude of average error. Here, RMSE has been implemented to estimate the performance of the proposed method. The square root of the average of squared differences between the outcomes of the proposed model and by the Kinect system have been measured to check the accuracy and efficiency. If the number of outcomes for a gait parameter is n, the outcome from the proposed prototype is O_p, and the outcomes from the Kinect is O_k over a given observation time t, then the RMSE is determined using the Eq. 5.

$$RMSE = \sqrt{\frac{1}{n}\sum_{t=1}^{n}(O_p - O_k)^2} \tag{5}$$

The angle between alternative thighs has been determined from both models (proposed and Kinect) and the accuracy of the gait study using UWB radar has been simultaneously measured through RMSE over a set observation time. The measurements have been performed in an anechoic chamber of the results shown in Figure 8.

V. Result Analysis

The comparative analysis of obtained results from the proposed prototype and Kinect sensor are demonstrated in this section. The processing of IR-UWB data and interpretation has been discussed in Section II-D which, explains the positions of back-scattered pulses from a human body and defines the motion through IR-UWB. Figure 6a displays one of the twenty normal walking pattern through IR-UWB response and 6b demonstrates the skeletonization of that gait pattern acquired from Kinect in anechoic chamber. Figure 6a shows a 3D structure looks like English letter 'W' which, includes the flexion and extension of skeletal muscle's (i.e., arm and legs) motion over the time. The skeletal muscles move faster than the other body sections which implies the transmission of higher energy by the bio-mechanical process that allows UWB radar to capture motion. The extension of lower limbs (left and right) makes separate motion area whereas, the flexion (right and leg) of lower limb and upper

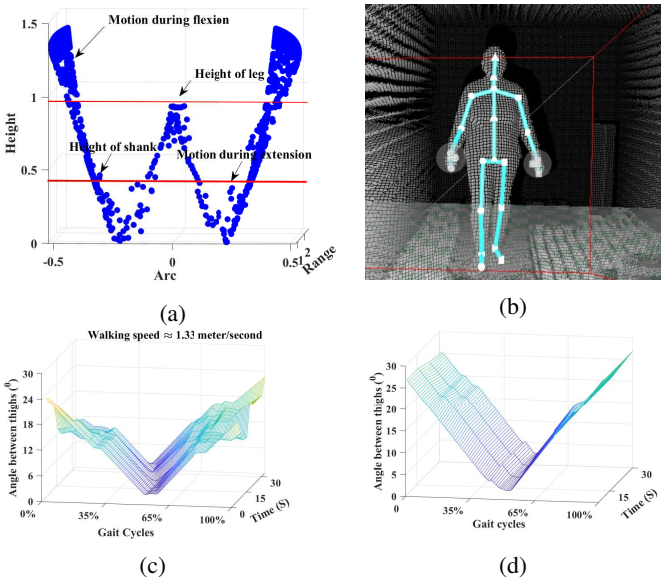

Fig. 6: The human motion and thigh angles obtained from proposed model and Kinect respectively for a person having normal walking pattern; (a) 3D human motion captured from IR-UWB, (b) 3D human skeleton captured from Kinect sensor, (c) Changes of thigh angles determined from proposed model, (d) Changes of thigh angles determined from Kinect skeleton.

limbs create a linear region from the shoulders that, explains the human motion. The person depicted in 6a and 6b has an actual height of that participant is 1.55 m whereas the estimated height of the shape is 1.35 m. This is because the model has captured all movements by UWB upto the height of shoulder from the ground level. The leg length of that participant is 0.95 m and knee height is 0.45 m that have been used to separate each lower limb sections for determining the angles between alternative thighs. Figure 6c and 6d demonstrates the estimation of thigh angles from proposed study and Kinect respectively using the method of Eq. 3 and Eq. 4. The x-axis denotes single gait cycle (in percentage) a person by considering two consecutive steps and the process has been repeated for 30 seconds plotted in y-axis and z-axis represents the angles between thighs during the observation time. The outcomes have been detailed here for 30 s for each participant. This participant has walked at a speed of 1.33 m/s (obtained from Doppler effect) and the thigh angles obtained from proposed prototype is approximately 24^0 whereas, the angles obtained from Kinect results approximately 26^0. The troughs represent here the angles during flexion and crest signifies the angles at the time of leg extension.

Figure 7 demonstrates the results acquired by experimenting one of the four persons having spastic gait. The same procedure like earlier has been employed to examine the spasticity. Figure 7b displays the left leg of the person is affected by spasticity. The stiffness of the left leg muscle forces the person to stretch the leg more during the walk

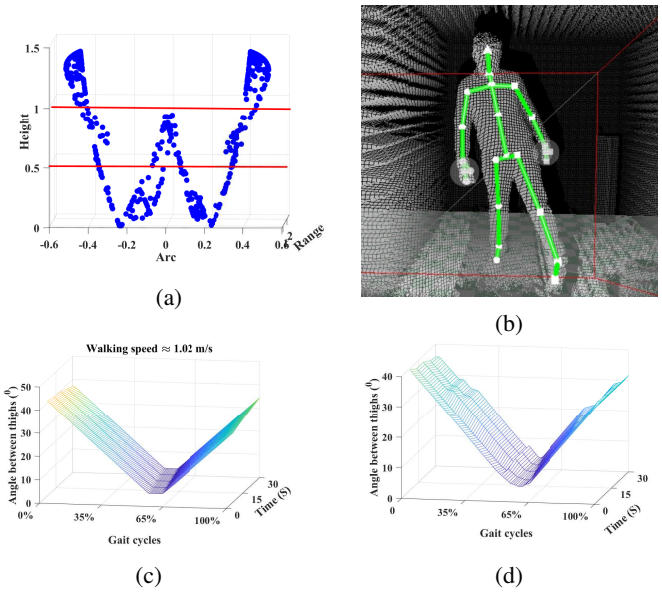

Fig. 7: The human motion and thigh angles obtained from proposed model and Kinect respectively for a person having spasticity; (a) 3D human motion captured by IR-UWB from spastic gait, (b) 3D human skeleton captured by Kinect sensor from spastic gait, (c) Changes of thigh angles determined from proposed model for spastic gait, (d) Changes of thigh angles determined from Kinect skeleton for spastic gait.

which, increases the angles between two thighs. Figure 7a shows that, the leg is deviated more from the center of body during the walk which, results the unusual thigh angle of approximately 40^0 determined from the proposed prototype. The angle between alternative thighs obtained from Kinect is approximately 38^0.

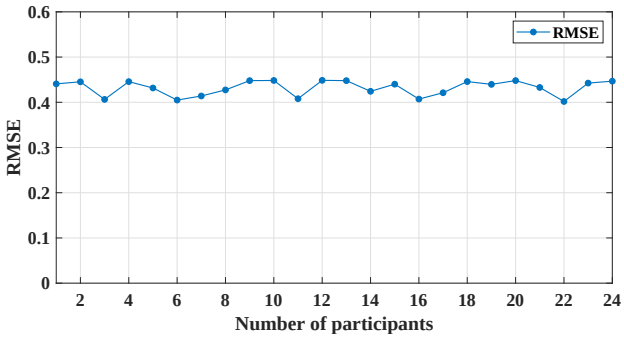

Fig. 8: RMSE of proposed outcomes against Kinect system outcomes.

To verify the outcomes RMSE (described in Section IV) have been implemented between the outcomes of proposed IR-UWB prototype and Kinect sensor. The RMSE scoring indicates the significant performance of the prototype. The error lies at the interval between 0.4 to 0.5 for all twenty four participants. The proposed prototype faces the error because, the height of lower limb has been considered for differentiation from the upper limb whereas, the arms come across the way of lower limb movements as a part of associated process and being detected as thigh movement.

VI. Conclusion

The proposed ITERATOR model intends to demonstrate a non-intrusive, non-contact, wireless for gait analysis and identification system capable and recognizing disorders related to human walking patterns. In this work, proposed 3D model of human motion has been generated from IR-UWB sensing for the first time by employing trigonometry and vector algebra where, subjective knowledge enable the study to further characterize human gait. This work is limited to identify the angles between thighs. The work is under way to determine further parameters to remote analyze gait such as, knee angles, step length, stride length, etc. In addition, greater number of participants including those with condition such as, propulsive, waddling, steppage, etc. would be considered for future experiment. The proposed model would be an cutting edge solution for addressing health issues by non-contact IR-UWB technology. Further, this study would be extended by employing supervised machine learning techniques to recognise the human walking disorders. This would provide a cutting-edge solution in health and medical perspective to assist in clinical and pathological gait diagnosis.

References

[1] K. Watanabe and M. Hokari, "Kinematical analysis and measurement of sports form," *IEEE Transactions on Systems, Man, and Cybernetics-Part A: Systems and Humans*, vol. 36, no. 3, pp. 549–557, 2006.

[2] S. Kimmeskamp and E. M. Hennig, "Heel to toe motion characteristics in parkinson patients during free walking," *Clinical biomechanics*, vol. 16, no. 9, pp. 806–812, 2001.

[3] A. Salarian, H. Russmann, F. J. Vingerhoets, P. R. Burkhard, and K. Aminian, "Ambulatory monitoring of physical activities in patients with parkinson's disease," *IEEE Transactions on Biomedical Engineering*, vol. 54, no. 12, pp. 2296–2299, 2007.

[4] K. M. Tsiouris, D. Gatsios, G. Rigas, S. Konitsiotis, A. Antonini, and D. I. Fotiadis, "A decision support system based on rapid progression rules to enhance baseline evaluation of parkinson's disease patients," in *Biomedical & Health Informatics (BHI), 2018 IEEE EMBS International Conference on*. IEEE, 2018, pp. 329–332.

[5] J. Li, X. Li, B. Yang, and X. Sun, "Segmentation-based image copy-move forgery detection scheme," *IEEE Transactions on Information Forensics and Security*, vol. 10, no. 3, pp. 507–518, 2015.

[6] P. Ren, S. Hu, Z. Han, Q. Wang, S. Yao, Z. Gao, J. Jin, M. L. Bringas, D. Yao, B. Biswal *et al.*, "Movement symmetry assessment by bilateral motion data fusion," *IEEE Transactions on Biomedical Engineering*, vol. 66, no. 1, pp. 225–236, 2019.

[7] P. Lopez-Meyer, G. D. Fulk, and E. S. Sazonov, "Automatic detection of temporal gait parameters in poststroke individuals," *IEEE Transactions on Information Technology in Biomedicine*, vol. 15, no. 4, pp. 594–601, 2011.

[8] J. R. Rebula, L. V. Ojeda, P. G. Adamczyk, and A. D. Kuo, "Measurement of foot placement and its variability with inertial sensors," *Gait & posture*, vol. 38, no. 4, pp. 974–980, 2013.

[9] A. Salarian, H. Russmann, F. J. Vingerhoets, C. Dehollain, Y. Blanc, P. R. Burkhard, and K. Aminian, "Gait assessment in parkinson's disease: toward an ambulatory system for long-term monitoring," *IEEE transactions on biomedical engineering*, vol. 51, no. 8, pp. 1434–1443, 2004.

[10] S. J. M. Bamberg, A. Y. Benbasat, D. M. Scarborough, D. E. Krebs, and J. A. Paradiso, "Gait analysis using a shoe-integrated wireless sensor system," *IEEE transactions on information technology in biomedicine*, vol. 12, no. 4, pp. 413–423, 2008.

[11] D. Tahmoush and J. Silvious, "Gait variations in human micro-doppler," *International Journal of Electronics and Telecommunications*, vol. 57, no. 1, pp. 23–28, 2011.

[12] J. Tana, M. Forss, and T. Hellstén, "The use of wearables in healthcare–challenges and opportunities," 2017.

[13] L. Piwek, D. A. Ellis, S. Andrews, and A. Joinson, "The rise of consumer health wearables: promises and barriers," *PLoS Medicine*, vol. 13, no. 2, p. e1001953, 2016.

[14] A. Pfister, A. M. West, S. Bronner, and J. A. Noah, "Comparative abilities of microsoft kinect and vicon 3d motion capture for gait analysis," *Journal of medical engineering & technology*, vol. 38, no. 5, pp. 274–280, 2014.

[15] S. P. Rana *et al.*, "UWB localization employing supervised learning method," in *IEEE 17th International Conference on Ubiquitous Wireless Broadband (ICUWB)*, Salamanca, Spain, 2017.

[16] S. Rana *et al.*, "Remote vital sign recognition through machine learning augmented UWB," in *IET 12th European Conference on Antennas and Propagation (EuCAP)*, London, United Kingdom, April, 2018.

[17] S. P. Rana, M. Dey, M. Ghavami, and S. Dudley, "Signature inspired home environments monitoring system using ir-uwb technology," *Sensors*, vol. 19, no. 2, 2019. [Online]. Available: http://www.mdpi.com/1424-8220/19/2/385

[18] F. C. Commission, "In the matter of revision of part 15 of the commission's rules regarding ultra-wideband transmission systems," *First Report And Order, ET Docket 98-153*, 2002.

[19] M. Hora, L. Soumar, H. Pontzer, and V. Sládek, "Body size and lower limb posture during walking in humans," *PloS one*, vol. 12, no. 2, p. e0172112, 2017.

[20] E. E. Stone and M. Skubic, "Unobtrusive, continuous, in-home gait measurement using the microsoft kinect," *IEEE Transactions on Biomedical Engineering*, vol. 60, no. 10, pp. 2925–2932, 2013.